Molecular Biology of the Cell
Vol. 14, 4997–5010, December 2003

Intersectin Regulates Fission and Internalization of Caveolae in Endothelial Cells

Sanda A. Predescu,* Dan N. Predescu,* Barbara K. Timblin,* Radu V. Stan,† and Asrar B. Malik*‡

*Department of Pharmacology, University of Illinois College of Medicine, Chicago, Illinois 60612; and †Department of Cellular and Molecular Medicine, School of Medicine, University of California, San Diego, La Jolla, California 92093

Submitted January 24, 2003; Revised July 25, 2003; Accepted July 26, 2003
Monitoring Editor: Keith Mostov

Intersectin, a multiple Eps15 homology and Src homology 3 (SH3) domain–containing protein, is a component of the endocytic machinery in neurons and nonneuronal cells. However, its role in endocytosis via caveolae in endothelial cells (ECs) is unclear. We demonstrate herein by coimmunoprecipitation, velocity sedimentation on glycerol gradients, and cross-linking that intersectin is present in ECs in a membrane-associated protein complex containing dynamin and SNAP-23. Electron microscopy (EM) immunogold labeling studies indicated that intersectin associated preferentially with the caveolar necks, and it remained associated with caveolae after their fission from the plasmalemma. A cell-free system depleted of intersectin failed to support caveolae fission from the plasma membrane. A biotin assay used to quantify caveolae internalization and extensive EM morphological analysis of ECs overexpressing wt-intersectin indicated a wide range of morphological changes (i.e., large caveolae clusters marginated at cell periphery and pleiomorphic caveolar necks) as well as impaired caveolae internalization. Biochemical evaluation of caveolae-mediated uptake by ELISA showed a 68.4% inhibition by reference to control. We also showed that intersectin interaction with dynamin was important in regulating the fission and internalization of caveolae. Taken together, the results indicate the crucial role of intersectin in the mechanism of caveolae fission in endothelial cells.

INTRODUCTION

Endothelial transcytosis, defined as the active transport of macromolecules across the endothelial barrier, rapidly and efficiently couples endocytosis to exocytosis of the transported molecules (Simionescu and Simionescu, 1991; Predescu *et al.,* 2001). Caveolae, the vesicular carriers mediating transcytosis, are abundant in ECs (Simionescu and Simionescu, 1984; Minshall *et al.,* 2000). They are released from the plasma membrane and form discrete vesicular carriers that shuttle between the two fronts of the cell, undergoing fusion-fission processes at each round of transport (Simionescu and Simionescu, 1991; Predescu *et al.,* 1997a; Niles and Malik, 1999). We showed that ECs possess the requisite "molecular machinery" for the repeated fusion-fission events involved in transcytosis; these components include SNAPs and SNAREs as well as caveolin-1, rab 5, dynamin, and lipids, organized in cytosolic supramolecular protein-lipid complexes (Predescu *et al.,* 1997b, 2001). The presence of dynamin, the membrane fission GTPase, in these complexes is of particular interest because it may be required for the highly specialized transcellular transport pathway in the endothelium. Previous studies have shown dynamin to be a critical determinant of caveolae fission in ECs (Oh *et al.,* 1998) and hepatocytes (Henley *et al.,* 1998).

Because intersectin is an important partner of dynamin in clathrin-dependent endocytosis (Hussain *et al.,* 1999; Pucharcos *et al.,* 2000), we surmised that intersectin might also be involved in caveolae internalization. Intersectins are members of a conserved family of proteins identified in humans (Guipponi *et al.,* 1998), rat (Okamoto *et al.,* 1999), mouse (Sengar *et al.,* 1999), *Xenopus laevis* (Yamabhay *et al.,* 1998), and *Drosophila melanogaster* (Roos and Kelly, 1998). Two highly similar intersectin genes, intersectin-1 and intersectin-2, have been identified, each producing two intersectin isoforms by alternative RNA splicing (O'Brian *et al.,* 2001). The short intersectins display two Eps 15 homology domains, a central coiled-coil region, and five consecutive SH3 domains (Guipponi *et al.,* 1998; Yamabhay *et al.,* 1998). Long intersectin-1, which is neuronal specific (Hussain *et al.,* 1999; Okamoto *et al.,* 1999), and long intersectin-2, with a wide mouse and human tissue distribution (Sengar *et al.,* 1999; Pucharcos *et al.,* 2000; O'Brian *et al.,* 2001), possess an extended COOH-region composed of DH (Dbl homology) domain, PH domain (pleckstrin homology), and C2 domain (Hussain *et al.,* 1999). Based on intersectin's interactions with dynamin (Hussain *et al.,* 1999; Okamoto *et al.,* 1999) and other endocytic proteins (Yamabhay *et al.,* 1998; Sengar *et al.,* 1999), it is possible that intersectin serves as a scaffolding protein regulating the assembly of multiprotein complexes at sites of formation of clathrin-coated vesicles (CCVs) and caveolae. Intersectin has also been proposed to couple endocytosis to exocytosis because its coiled-coil domain binds to SNAP-23 and SNAP-25 (Okamoto *et al.,* 1999). Because

Article published online ahead of print. Mol. Biol. Cell 10.1091/mbc.E03–01–0041. Article and publication date are available at www.molbiolcell.org/cgi/doi/10.1091/mbc.E03–01–0041.

† Corresponding author. E-mail address: abmalik@uic.edu.

Abbreviations used: CCPs, clathrin-coated pits, CCVs, clathrin-coated vesicles; CT, cholera toxin; DN-dominant negative, DNP, dinitrophenyl; ECs, endothelial cells; PBSo, phosphate-buffered saline + 0.2% ovalbumin.

intersectin can activate mitogenic signaling pathways, it may provide a molecular link between endocytosis and the mitogenic machinery (Adams *et al.*, 2000). In addition, long intersectin isoforms can stimulate actin assembly by Cdc42 activation of N-WASP (Wiscott-Aldrich syndrome protein) and Arp2/Arp3 complex (McPherson, 2002).

We investigated using cultured ECs the expression and subcellular localization of intersectin and addressed intersectin's involvement in caveolae fission and internalization. ECs provide a highly suitable system to address these questions because of their numerous caveolae and high transcytotic activity. We have for the first time localized intersectin to the caveolae neck region; thus, through its strategic location and ability to bind simultaneously more dynamin molecules, it appears that intersectin recruits dynamin to generate a high local concentration required for collar formation, and caveolae fission and internalization. Our results provide biochemical and morphological evidence demonstrating that the intersectin-dynamin interaction is crucial in the mechanism of fission and internalization of caveolae.

MATERIALS AND METHODS

Materials

Lung human microvascular ECs were obtained from Clonetics (San Diego, CA) and Sprague-Dawley rats were bought from the Harlan-Sprague Laboratories (Indianapolis, IN). EZ-Link Sulfo NHS-SS-Biotin from Fisher Scientific (Hanover Park, IL), cholera toxin (CT) biotin or FITC-labeled from Sigma (St. Louis, MO), X-OMAT Blue XB-1 film from NEN Life Science Products (Boston, MA), blasticidin S HCl from Invitrogen (Carlsbad, CA), FuGENE 6 Transfection reagent from Roche Molecular Biochemicals (Indianapolis, IN), Prolong Antifade kit, and NeutrAvidin Texas Red conjugated from Molecular Probes (Eugene, OR), protein A/G agarose from Santa Cruz Biotechnology (Santa Cruz, CA), and streptavidin-HRP conjugated, MicroBCA (bicinchoninic acid) Protein Assay Reagent Kit, disuccinimidyl tartrate (DST), and SuperSignal Chemiluminescent Substrate from Pierce (Rockford, IL). All EM grade reagents were from EM Science (Forth Washington, PA). All other reagents were from Sigma if not otherwise specified.

Relevant antibodies were obtained from the following sources: anti-intersectin polyclonal antibody (pAb) was a gift from Dr. Thomas Südhof (Southwestern Medical School, Dallas, TX), anti-dynamin and anti-caveolin mAbs from Transduction Laboratories (Lexington, KY), anti-dynamin pAb from Cell Signaling Technology (Beverly, MA), anti-SNAP-23 pAb from Synaptic Systems (Göttingen, Germany), HRP-conjugated anti-mouse IgG and HRP-conjugated anti-rabbit IgG from Cappel, Organon Teknika (Durham, NC), anti-mouse IgG-FITC and anti-rabbit IgG-Texas Red from Jackson ImmunoResearch (West Grove, PA). Anti–caveolin-1 pAb and anti-myc mAb were prepared as described (Stan *et al.*, 1997). Colloidal gold suspensions were prepared as in Slot and Geuze (1985), stabilized with protein A or streptavidin (Quagliarello *et al.*, 1991), and stored as concentrate at 4°C. Rabbit IgG dinitrophenyl (DNP) conjugated was prepared as described (Predescu *et al.*, 1997a).

Endothelial Cell Culture

ECs seeded in 100-cm^2 plastic Petri dishes were grown to confluence in medium 199 supplemented with 20% fetal calf serum. To verify their endothelial identity and degree of differentiation, the presence of factor VIII-antigen was assessed by indirect immunofluorescence, and the presence of Weibel-Palade bodies was checked by EM.

Protein Extraction

Cell lysates were prepared at 4°C using an extraction buffer containing 20 mM HEPES/KOH, pH 7.4, 2% Triton X-100, 100 mM KCl, 2 mM DTT, 2 mM EDTA, and 1 mM PMSF. Confluent EC monolayers were treated with 1 ml extraction buffer for 30 min, at RT, under gentle agitation. The cell monolayer was scraped with a rubber policeman, and the ensuing lysate was clarified by centrifugation in a Beckman TLA ultracentrifuge with a TLA-45 rotor, for 60 min at 40,000 rpm. Rat lung lysate was prepared as described (Predescu *et al.*, 1995). Protein concentration was determined by the BCA micromethod with a BSA standard.

Immunoprecipitation and Immunoblotting

For immunoprecipitation studies, 100 μg total protein from the ECs or rat lung lysates were precleared using a rabbit IgG followed by protein A/G agarose beads, for 1 h each, at RT. The resulting supernatant was incubated overnight, at 4°C with affinity-purified anti-intersectin, anti-SNAP-23 pAbs, or anti-dynamin mAb, followed by incubation 1 h, at RT with protein A/G. Beads were washed extensively, and after solubilization in electrophoresis sample buffer, the immunoprecipitates were resolved on 5–20% SDS PAGE, electro-transferred to nitrocellulose membranes, and analyzed by immunoblotting.

Cross-linking Experiments Using DST

The cross-linking reaction was started by applying directly DST, a membrane-permeant cross-linker, periodate cleavable, on undisrupted ECs, according to the manufacturer's instructions. The specific cross-linked products were analyzed after immunoprecipitation with anti-dynamin mAb by two-dimensional gel electrophoresis as described (Smith et al., 1978; Predescu et al., 2001).

Immunofluorescence Microscopy

Confluent ECs monolayers grown on glass coverslips and washed in PBS (five times for 2 min) were fixed (methanol, 10 min, −20°C), quenched (PBS + 1% BSA; 1 h, RT), and incubated in the appropriate first antibody diluted in PBS + 0.1% BSA. After washing (PBS + 0.1% BSA; five times for 5 min), the cells were reacted for 1 h, at RT, with the reporter antibodies, washed again as above, and then mounted on glass slides using ProLong Antifade kit, examined, and photographed in a Zeiss Axiophot 20 microscope (Thornwood, NY).

When internalization of biotinylated cell surface proteins was examined, control or transfected ECs grown on glass coverslips were incubated as above for 1 h, at RT with anti-myc mAb (Predescu et al., 2001), to detect the myc-tagged exogenous protein. NeutrAvidin-Texas Red, used to visualize biotin-labeled proteins and anti-mouse IgG-FITC, used to detect the bound myc antibody, were applied together, for 1 h, at RT.

Electronmicroscopy

The distribution of intersectin and dynamin within streptolysin O (SLO)-permeabilized cultured ECs was examined by EM immunogold labeling via DNP-conjugated IgG and Protein A-gold as in Pathak and Anderson (1989), slightly modified by us. DNP epitope resists EM fixation and Epon embedding and can be detected efficiently by anti-DNP antibody on the surface of thin-sectioned specimens. ECs grown in 35-mm plastic Petri dishes were washed (PBS; three times for 2 min), fixed (PBS containing 2% paraformaldehyde and 0.2% glutaraldehyde; 30 min, RT), washed again (PBS + 0.2% ovalbumin [PBSo], three times for 2 min), collected by gentle centrifugation in PBSo, and permeabilized with SLO as in Predescu *et al.* (2001). Briefly, the cells suspended in PBSo were incubated with 40 HU (hemolytic units) SLO/ml, for 5 min on ice followed by 15 min at 37°C. After permeabilization, the cells were pelleted by gentle centrifugation, washed three times in PBSo, and then reacted with anti-intersectin or anti-dynamin pAbs diluted in the same buffer, for 2 h, at RT. The specificity of the antibody labeling was demonstrated using a nonspecific, isotype-matching antibody or by omitting anti-intersectin or anti-dynamin antibodies. After washing (PBSo, five times for 5 min), the cells were reacted with anti-rabbit IgG-DNP diluted in PBSo for 1 h, at RT. The cells were again washed, fixed with 0.2% glutaraldehyde in PBS, and the cell pellet was subjected to the standard EM procedure (Predescu *et al.*, 1997a). Thin sections cut from blocks mounted on nickel grids were quenched with PBS containing 0.1 M glycine and 1% BSA, (10 min), blocked with 1% BSA, 0.1% gelatin in PBS for 15 min, and then incubated (2 h, RT) with anti-DNP mAb, diluted in 1% BSA in PBS. The grids were washed (five times for 3 min), in 0.1% BSA in PBS, and (two times for 5 min) in PBS + 1% BSA, incubated for 1 h with protein A-gold diluted in 0.1% BSA in PBS to an $OD_{520\ nm}^{Au} = 0.2$, washed again (0.1% BSA in PBS; five times for 3 min), stained with uranyl acetate and lead citrate, and finally examined and micrographed in a Philips (Hillsboro, OR) CM-10 transmission EM.

Morphometric Analysis

The number of gold particles associated with caveolae and other endothelial structures were counted and normalized per 10 μm^2 of EC surface. We used 212 randomly chosen micrographs (×84,000 final magnification) to count the total number of gold particles as well as the number of caveolae open to the cell surface or apparently free in the cytosol.

For the analysis of morphological changes induced by intersectin overexpression, 15–20 sections per grid and 3–5 grids/ per block from 10 Epon blocks, chosen at random, for control or transfected cells, were used. The morphological appearance (vesicles open apically, basolaterally, or apparently free in the cytosol) was recorded on 100 micrographs (×98,000 standard magnification) for each experimental condition.

Caveolae Fission Assays

Sheets of endothelial luminal membranes bearing attached caveolae were prepared and purified as described (Stan *et al.*, 1997). Before use in the fission assay, the membrane sheets were subjected to high-salt treatment (1 M KCl)

to remove the membrane-associated pool of intersectin, and aliquots were checked by immunoblotting to confirm intersectin depletion. Once prepared, plasma membrane patches were incubated for 1 h, at 37°C with EC cytosol in the presence of 1 mM GTP, and an ATP-regenerating system (1 mM ATP, 10 U/ml creatine phosphokinase and 10 mM phosphocreatine), conditions that induce caveolae release from plasma membrane patches (Schnitzer *et al.*, 1996). Caveolae release was monitored biochemically by sucrose density centrifugation as described (Oh *et al.*, 1998). The protocol has been complemented by morphological analysis of the light-membranes fractions obtained on sucrose gradients and by immunogold labeling and negative staining EM as described (Predescu *et al.*, 2001). The cytosolic fraction obtained by SLO permeabilization of EC membranes (Predescu *et al.*, 2001) was depleted for intersectin using specific antibodies against intersectin, followed by protein A/G. This step was repeated until Western blotting analysis of this cytosol fraction indicated no detectable intersectin staining. The specificity of intersectin immunodepletion was confirmed using an isotype specific IgG.

Internalization Assay

Transfected cells grown on plastic Petri dishes or glass coverslips were washed with ice-cold PBS and then incubated with 0.5 mg/ml cleavable biotin reagent as described in Zurzolo et al. (1994) or 20 nm CT-biotin (Lencer *et al.*, 1992). Biotinylated cell surface proteins and CT-biotin, respectively, were internalized for 30 min, at 37°C. Biotinylated proteins still at the cell surface after 30 min were reduced with glutathione (Bretscher and Lutter, 1988) and the cells were further processed for morphological analysis or lysed for biochemical investigation. The efficiency of reduction reaction was 97% (as calculated by comparing total amount of biotinylated proteins at the cell surface before internalization to amount of biotinylated proteins still on the cell surface after applying the reducing solution).

For biochemical studies, control or transfected cells were lysed in TBS containing 2% Triton X-100, and the lysates were clarified by centrifugation for 30 min, at 4°C, 40,000 rpm in a TLA-45 Beckman (Fullerton, CA) rotor, to obtain a final supernatant expected to contain the biotinylated proteins internalized by control or transfected ECs. The amounts of biotin labeled proteins were assessed by ELISA (Savage *et al.*, 1992). For quantitative assessment of biotin molecules in the final EC supernatant, standard curves were generated using known concentrations of BSA-biotin and CT-biotin. The average number of biotin molecules present in each cell lysate was determined at a series of decreasing concentrations from the linear part of the curve obtained by successively diluting a standard volume (100 μl) from each lysate and normalized per mg total protein.

K^+ Depletion Experiments

Depletion of intracellular K^+ was performed by incubation of ECs for 5 min with hypotonic medium followed by transfer to isotonic K^+-free buffer as described (Larkin *et al.*, 1983).

Intersectin Constructs and Transfection Procedure

Full-length *Xenopus laevis* intersectin cDNA clone pCEN-HA-Itsn (Gift from Dr. B.B. Kay, University of Wisconsin, Madison, WI), was used as a template for PCR with PFU (Stratagene, La Jolla, CA), DNA polymerase to generate C-terminal Myc-His–tagged proteins that are either full length or SH3A domain deleted. Primer pair IntF; 5′-CTCCGGTACCAAACC**ATG**GCTCAGTTTGGAACTCC-3′::IntR; 5′-CCTAGGCCTCGAGTATATTTATATATTTTACATTC-3′ was used to generate a full-length intersectin cDNA that lacks the stop codon. The resulting PCR fragment was cloned into pCR4Blunt-TOPO vector (Invitrogen) and subsequently subcloned into the *Kpn*I-*Xho*I restriction sites (underlined in primers) of pcDNA6/Myc-His A, resulting in vector pInt-MycHis. Deletion of the SH3A domain A was performed through a two-step "spliced overhang extension" PCR as outlined (Anderson *et al.*, 1998). Briefly, first-step PCR products generated using primer pairs Int(ΔSH3A)F; 5′-CAACCAGGGCGATAGTGAATTTCCAAGCAC-3′::IntR and Int(ΔSH3A)R;

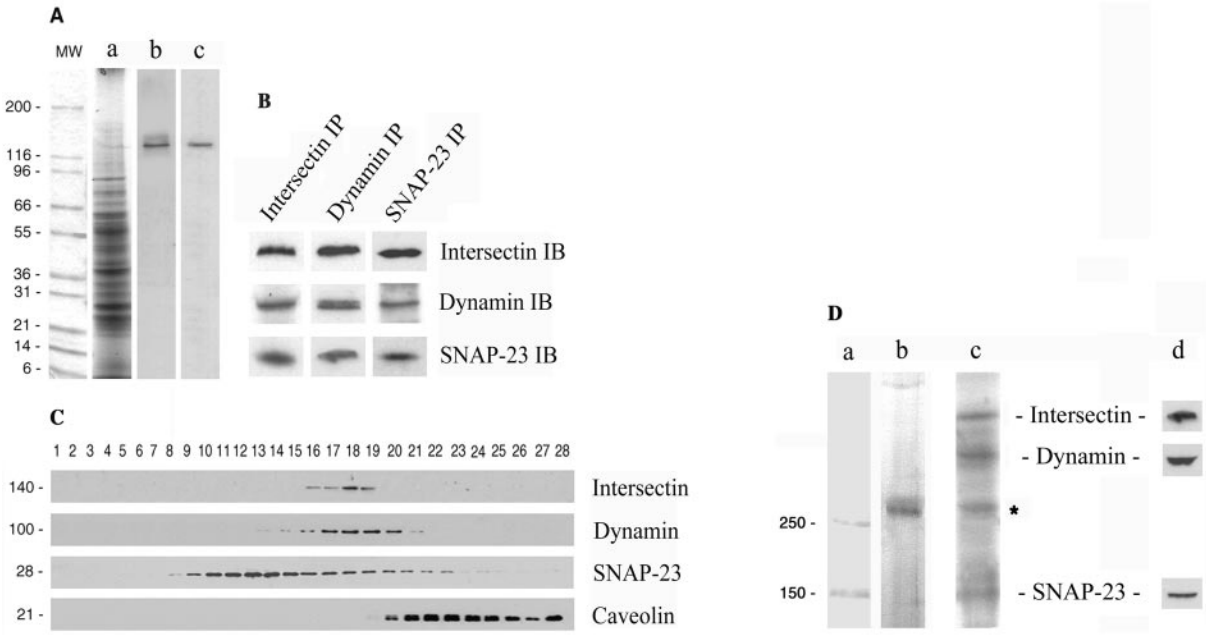

Figure 1. Intersectin is present in ECs in a membrane-associated protein complex containing dynamin and SNAP-23. (A) Western blotting of cultured ECs (b) and rat lung (c) detergent extracts using affinity-purified anti-intersectin pAb shows a band of immunoreactivity of ~140 kDa. (a) Coomassie staining of total EC lysate. MW, protein standards. (B) Immunoprecipitation analysis applied on cultured EC lysates using the specific anti-intersectin, anti-dynamin, and anti-SNAP-23 antibodies indicates the presence of the same endothelial proteins in the immunoprecipitate. (C) Total protein (500 μg) from EC lysate was subjected to 10–35% glycerol gradient centrifugation, at 4°C, 42,000 rpm, overnight, in a SW55 Beckman rotor. Fractions (28 fractions of 180 μl each) were collected. Aliquots (20 μl) from each fraction were subjected to SDS-PAGE, followed by Western blotting using each indicated antibody. The similar sedimentation pattern indicates that intersectin is a protein component of a complex containing dynamin and SNAP-23 in ECs, whereas caveolin-1 is not part of this complex. An ECL detection system was used in all cases to visualize the bound antibodies. All results above are representative of four separate experiments. (D) The cross-linked products generated by DST in intact cultured ECs were immunoprecipitated with anti-dynamin mAb and analyzed by 6% SDS-PAGE in 8 M urea. Commassie R-250 staining indicated the presence of an aggregate >250 kDa (b) only in the membrane fraction. Second-dimensional analysis of the cross-linked product on 10% SDS-PAGE followed by silver staining suggests the presence of intersectin, dynamin, and SNAP-23 complex. The identity of the 70-kDa protein (*) is unknown. (c) Immunoblotting analysis with anti-intersectin, anti-dynamin, and anti–SNAP-23 pAbs confirmed the identity of the protein bands (d). MW standards (a) apply only to lane b.

5′-TGGAAATTCACTATCGCCCTGGTTGATC-3′::IntF were mixed, and complementary ends were annealed to generate a double-stranded DNA fragment that was amplified using primer pair IntF::IntR in the second-step PCR. The resulting PCR product was cloned into the pCR4Blunt-TOPO vector and subsequently subcloned into the *Eco*RI-*Xho*I restriction sites of pcDNA6/Myc-His A, resulting in a vector pInt(ΔSH3A)-MycHis. To generate a Myc-His–tagged dominant negative mutant, primer pair XInt-SH3F; 5′-CAGAATTCACC**ATG**GTGAAGGTTGTGTATTACC-3′: XInt-SH3R; 5′-CCTAGGCCTCGAGGTCTGTGGTCAGTTTCAC-3′ was used to amplify the entire SH3 domain of intersectin. The PCR product was cloned in frame into the *Eco*RI-*Xho*I restriction sites (underlined in primers) of pcDNA6/Myc-His, resulting in vector pInt-SH3MycHis. The translational start codon is given in boldfaced letters. All clones were sequenced to ensure sequence integrity. All transfections were performed using FuGENE 6 transfection reagent, according to the manufacturer's instructions.

RESULTS

Expression of Intersectin in ECs

Expression of intersectin was investigated by immunoblotting of cultured ECs and rat lung detergent extracts with affinity-purified anti-intersectin pAb (Okamoto *et al.*, 1999). A band of immunoreactivity of 140 kDa was observed in both cases, in agreement with the predicted M_r of short intersectin (Figure 1A). In this study, we will refer to short intersectin-1 as intersectin. To analyze the interactions of intersectin with endothelial proteins, we performed immunoprecipitation analysis of EC lysate using anti-intersectin pAbs. Both dynamin and SNAP-23 coimmunoprecipitated with intersectin as detected with specific antibodies (Figure 1B). The same interactions were detected when anti-dynamin mAb or anti-SNAP-23 pAb were used for immunoprecipitation (Figure 1B). None of these proteins was found in the immunoprecipitate using an isotype-specific rabbit IgG for immunoprecipitation (our unpublished results). To further characterize these interactions, we applied velocity sedimentation on glycerol gradients. Aliquots from each fraction were analyzed by SDS-PAGE, electro-transferred to nitrocellulose membranes, and immunostained with antibodies against intersectin, dynamin, SNAP-23, and caveolin-1. As shown in Figure 1C, intersectin, dynamin, and SNAP-23 displayed similar distribution patterns. Intersectin and dynamin were mostly recovered in fractions 16–19, whereas the t-SNARE, SNAP-23, displayed a wider distribution along gradient fractions. All three proteins showed, as indicated by immunoblotting, a comparable quantitative distribution in fractions 16–19. In contrast, caveolin-1 was recovered primarily in fractions 20–28. Independent evidence of intersectin-dynamin-SNAP-23 interaction was obtained by cross-linking with DST, a membrane-permeant cross-linker, applied to intact cultured ECs (Figure 1D). The cross-linked products of interest generated by DST were immunoprecipitated with anti-dynamin pAb from cytosol and membrane fractions prepared by SLO-permeabilization of the cell membrane (Predescu *et al.*, 2001). The immunoprecipitate was analyzed by 6% SDS PAGE containing 8 M urea. A cross-linked aggregate greater than 250-kDa, as detected by Commassie R-250 staining only in the membrane fraction (Figure 1D, lane b), was subjected to a second dimensional analysis (Predescu *et al.*, 2001). The protein profile obtained by silver staining (Figure 1D, lane c) showed four major protein bands; three of them were identified by immunoblotting as SNAP-23, dynamin, and intersectin (Figure 1D, lane d). The identity of the 70-kDa protein band is unknown. Although both intersectin and dynamin are also present in soluble pools, soluble cross-linked aggregates were not detected. On the basis of these findings, we conclude that intersectin, dynamin, and SNAP-23 form a membrane-associated complex in ECs.

Subcellular Localization of Intersectin

Immunofluorescence labeling of cultured ECs using anti-intersectin pAb indicated intense punctate staining at the cell surface and throughout the cytosol (Figure 2), suggesting intersectin association with vesicle-like structures, probably caveolae. Indeed, double immunofluorescent staining using both anti-intersectin pAb (Figure 2Aa) and anti-caveolin mAb (Figure 2Ab) indicated a considerable colocalization of the two probes (2A, c and inset c1), both intracellular and at the plasma membrane. On the basis of the biochemical evidence for intersectin-dynamin interaction, we also examined their subcellular distribution by fluorescence microscopy. Anti-dynamin mAb revealed a punctate pattern that overlapped a predominant diffuse staining (Figure 2Bb). Detailed punctate intersectin and dynamin staining is shown in Figure 2B, insets a1 and b1, respectively. The merged image showed significant colocalization (Figure 2Bc), but did not exclude the presence of structures labeled by only one probe (Figure 2Bc, inset).

We used immunogold labeling to gain more insights into the association of intersectin with cell structures within ECs.

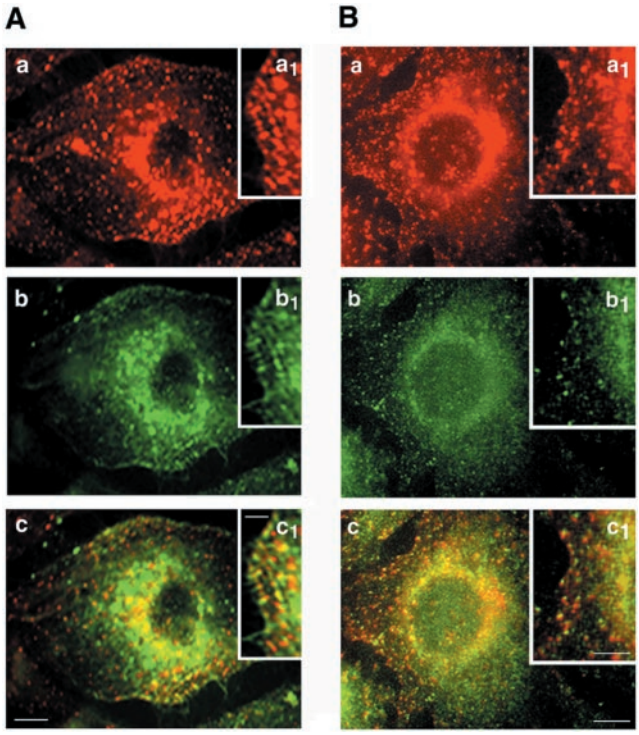

Figure 2. Subcellular distribution of intersectin by double immunofluorescence in cultured ECs. Intersectin displays a punctate staining pattern both at the plasma membrane and throughout the cytoplasm in cultured ECs permeabilized by methanol fixation (A and B, red staining, a and a1). (A) Caveolin immunostaining in cultured ECs (b). The merged image (c) indicated extensive colocalization of the signals for intersectin and caveolin (panel c and inset c1), both intracellular and at the plasma membrane. (B) Anti-dynamin mAb revealed a similar punctate pattern that overlapped a predominant diffuse pattern (b). The merged image (c) indicates marked colocalization of intersectin (red) and dynamin (green) both at the plasma membrane and cytoplasm of an EC. Insets a_1 and b_1 show in detail the punctate intersectin and dynamin staining at the plasma membrane. The majority of the reactive small vesicles at the plasma membrane contain both proteins (c_1). Results are representative of three experiments. Bars, (a–c) 10 μm; (insets) 5 μm.

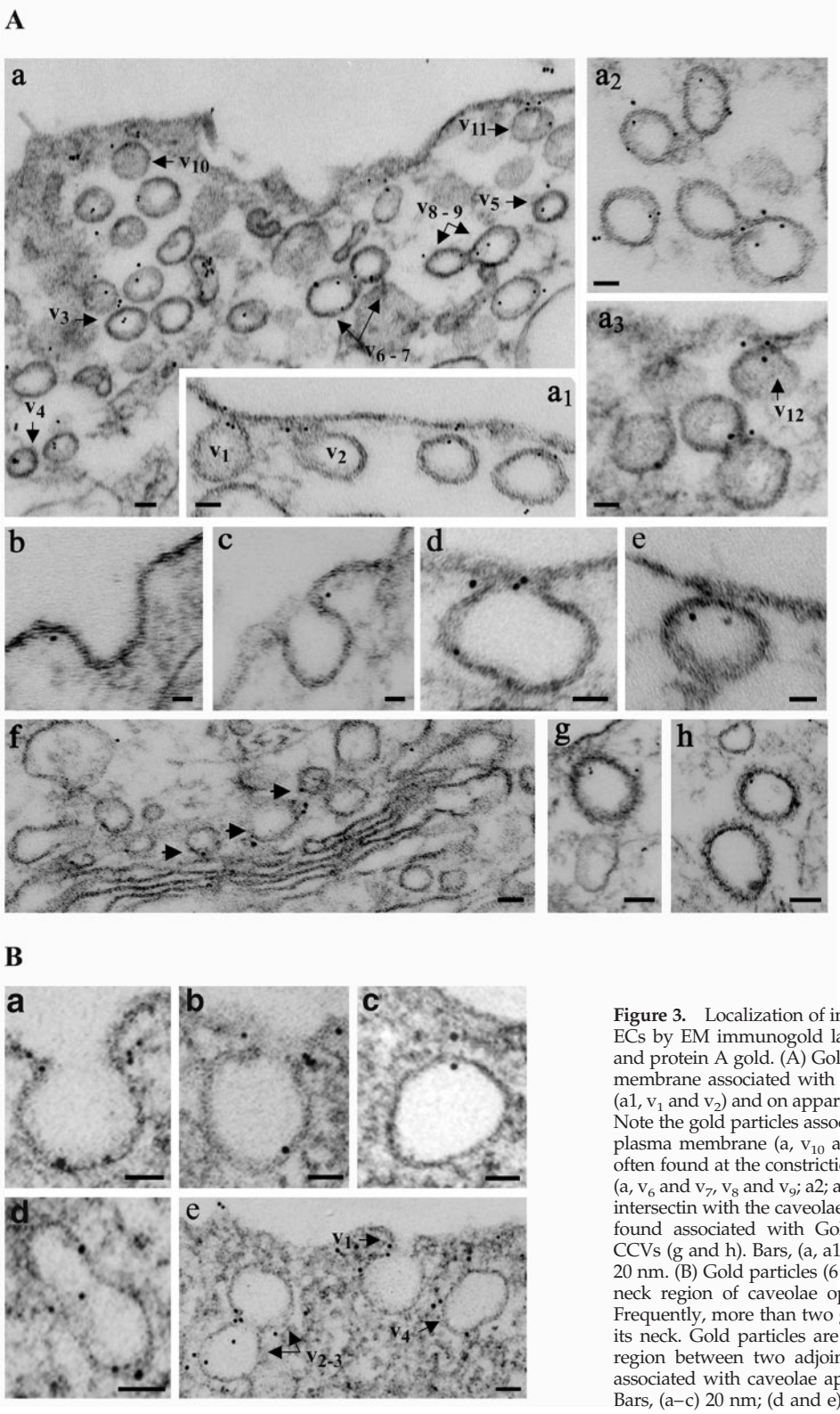

Figure 3. Localization of intersectin (A) and dynamin (B) in cultured ECs by EM immunogold labeling using DNP-conjugated rabbit IgG and protein A gold. (A) Gold particles (5 nm) are found at the plasma membrane associated with caveolae profiles open to the apical front (a1, v_1 and v_2) and on apparently free caveolae in the cytosol (a, v_3–v_5). Note the gold particles associated with caveolae just released from the plasma membrane (a, v_{10} and v_{11}; a3, v_{12}; and e). Gold particles are often found at the constriction region between two adjoining caveolae (a, v_6 and v_7, v_8 and v_9; a2; and a3). Note the preferential association of intersectin with the caveolae neck region (b–d). Gold particles are also found associated with Golgi-derived vesicles (f, arrowheads) and CCVs (g and h). Bars, (a, a1, a2, a3, f, g, and h) 50 nm, (b, c, d, and e) 20 nm. (B) Gold particles (6 nm) are preferentially associated with the neck region of caveolae open to the EC surface (a, b, and e, v_1). Frequently, more than two gold particles labeled a caveolar profile or its neck. Gold particles are also frequently found at the constriction region between two adjoining caveolae (d and e, v_1 and v_2) and associated with caveolae apparently free in the cytosol (c and e, v_3). Bars, (a–c) 20 nm; (d and e) 50 nm.

Anti-intersectin pAb applied to fixed and SLO-permeabilized cells was detected with DNP anti-rabbit IgG, followed by anti-DNP mAb and protein A-gold (Pathak and Anderson, 1989), modified as described in MATERIALS AND METHODS. We found intersectin, under conditions of good endothelial morphology and large sampling, at the plasma membrane (Figure 3A) specifically associated with caveolae open to the cell surface, (a1–v_1, v_2). Notably, intersectin was

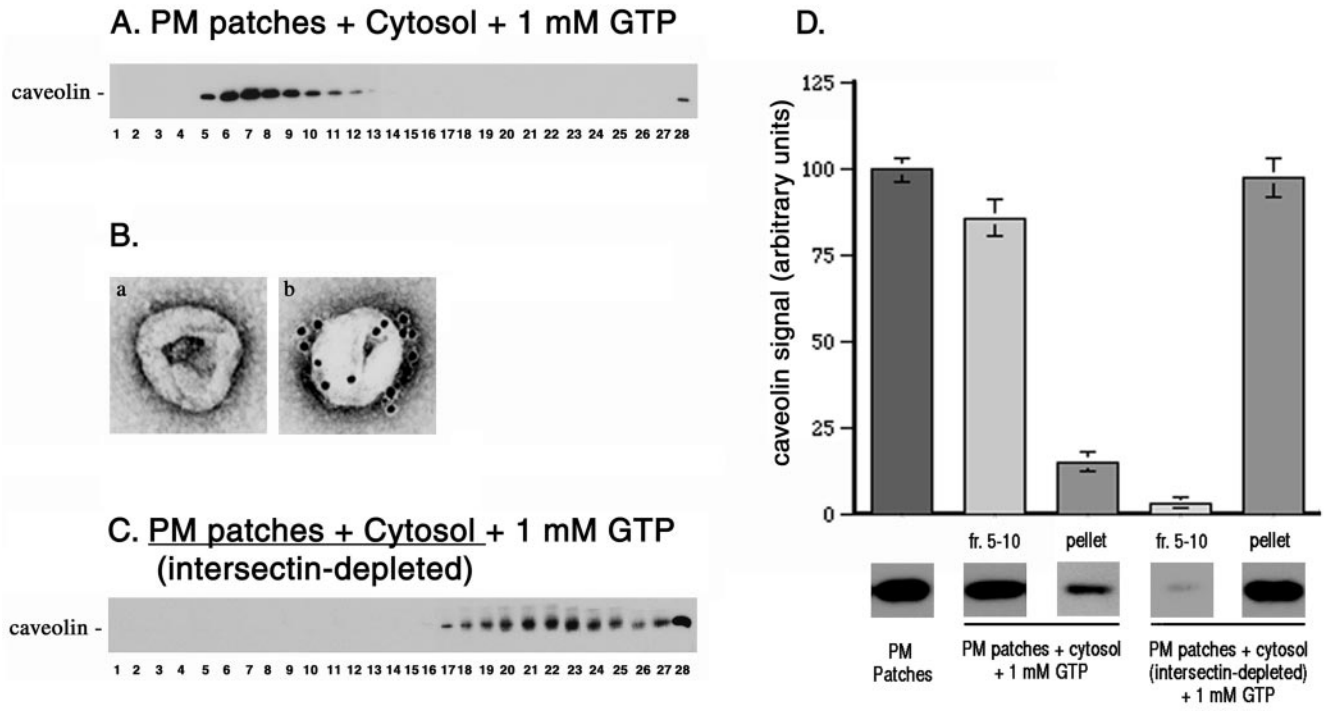

Figure 4. Intersectin is required for caveolae fission. (A) Low-density caveolin-enriched membranes (fractions. 5–11) were obtained by density centrifugation on sucrose gradients when rat lung EC plasma membrane patches bearing attached caveolae were incubated with cytosol, 1 mM GTP, and the ATP regenerating system. (B) EM negative staining applied on aliquots from fraction 7 of sucrose gradients revealed a homogeneous population of caveolae (a), which by EM immunocytochemistry were heavily labeled by 10 nm gold conjugated anti-caveolin pAb (b). (C) When both cytosol and plasma membranes sheets were depleted in intersectin, caveolin was not detected by Western blotting in the light fractions of sucrose gradients. The GTP-induced caveolae fission did not occur. (D) The signal detected for caveolin by immunoblotting of aliquots containing equal amounts of total protein from PM patches (starting material), fractions 5–10 of sucrose gradients, and repelleted silica-coated membranes, were quantified by scanning densitometry and plotted as a percentage of signal detected in the starting material. All data are representative for four different experiments.

preferentially associated with the neck region of wide or narrow open caveolae (b, c, d). Intersectin was also frequently associated with apparently free caveolae, (a–v_3, v_4, v_5, a2) and with the constricted region of two adjoining caveolae (a–v_{6-7}, v_{8-9}). Morphometric analysis indicated that 38% of the 612 gold particles counted on 10 μm^2 of EC surface labeled caveolae open to the cell surface, whereas 23% were found on caveolae apparently free in the cytosol. Interestingly, ~87% of gold particles labeling caveolae open to the cell surface were exclusively associated with their neck region. Gold particles were also associated with CCVs (Figure 3 A, g and h). These data (summarized in Table 1) provide the first EM morphological evidence of intersectin association with caveolae and CCVs, and its preferential association with caveolar neck. Small clusters of gold particles were also present throughout the cytosol (19%), on Golgi-derived vesicles, and associated with cytoskeletal elements (8%; Figure 3Af).

We took advantage of this methodology to examine dynamin distribution in cultured ECs. As reported (Oh *et al.*, 1998), we found dynamin (Figure 3 B) preferentially associated with the neck region of caveolae (a, b, e–v_1). However, we also found gold particles associated with the constricted region between two adjacent caveolae (d, e–v_{2-3}) and with caveolae apparently free in the cytosol (c, e–v_4), implying that some dynamin remains associated with caveolae after

Table 1. Morphometric analysis of intersectin localization in cultured ECs by EM immunogold labeling

	Caveolae					
	Plasma membrane[a]	Cytosol	Plasmalemma proper	Cytosol	CCVs	ICM
Gold particles	232 ± 12	141 ± 10	37 ± 8	116 ± 13	37 ± 5	49 ± 6
Intersectin labeling (%)	38	23	6	19	6	8

On 10 μm^2 of EC surface containing 396 caveolar profiles, we counted 612 gold particles; 61% of gold particles were associated with caveolar profiles. CCVs, clathrin-coated vesicles; ICM, intracellular membranes. Data are shown as means ± SD.

[a] From 232 gold particles counted on caveolae open to the cell surface, 202 particles (~87%) were associated with the caveolar neck region.

detachment from plasmalemma. Morphometric analysis of dynamin immunogold labeling showed that of the 632 gold particles found on 10 μm^2 of EC surface, 442 particles (70%) were associated with caveolae, whereas the remaining 190 were found in the cytosol (14%), on the plasmalemma proper (11%), or other intracellular membranes (5%). About 272 gold particles (86%) detected on caveolae open to the cell surface were associated with the caveolae neck region. Taken together, the findings suggest that the intersectin-dynamin association may provide a highly efficient control of caveolae release from the plasma membrane and caveolae clusters during transcytosis.

Intersectin Is Required for Caveolae Fission

To address the functional relationship between intersectin and caveolae, we used a cell-free system for caveolae fission (Schnitzer *et al.*, 1996) modified as described in MATERIALS AND METHODS. In controls, purified rat lung endothelial

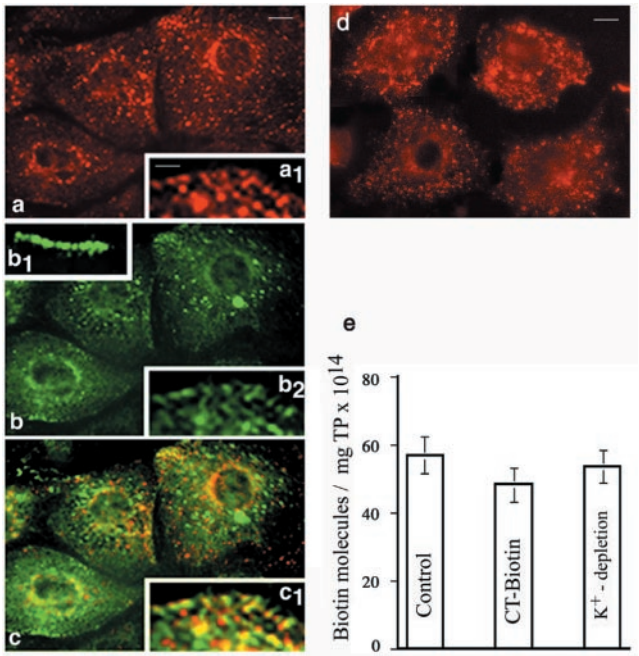

Figure 5. Internalization of biotinylated cell surface proteins in ECs by caveolae. Contribution of caveolae to the internalization of biotinylated cell surface proteins was evaluated using a double internalization assay and CT-FITC as a marker for the caveolar uptake. Cell surface proteins were biotinylated and then internalized for 30 min, at 37°C. Biotinylated proteins still on the cell surface after 30 min were reduced with glutathione, and the uptake of biotinylated surface proteins was analyzed morphologically by fluorescence microscopy using neutrAvidin-Texas Red (a). CT-FITC bound on the cell surface at 4°C (inset $b_{.1}$) was internalized for 30 min at 37°C (b). Virtually similar staining pattern indicates the dominant contribution of caveolae to the internalization process. The merged image (c) indicates the degree of colocalization of the two probes. Inset c.1 shows in detail that majority of small vesicles contain both probes. Results are representative of three experiments. Bars, (a–c) 10 μm; (insets) 4 μm. (d) K^+ depletion used to inhibit internalization by CCVs did not affect caveolae internalization. (e) The number of biotin molecules in the final supernates of ECs lysates when biotinylated cell surface proteins or CT-biotin were used as probes. A similar number of biotin molecules are found in the lysates of ECs K^+-depleted. Results are the averages ± SD of four different experiments.

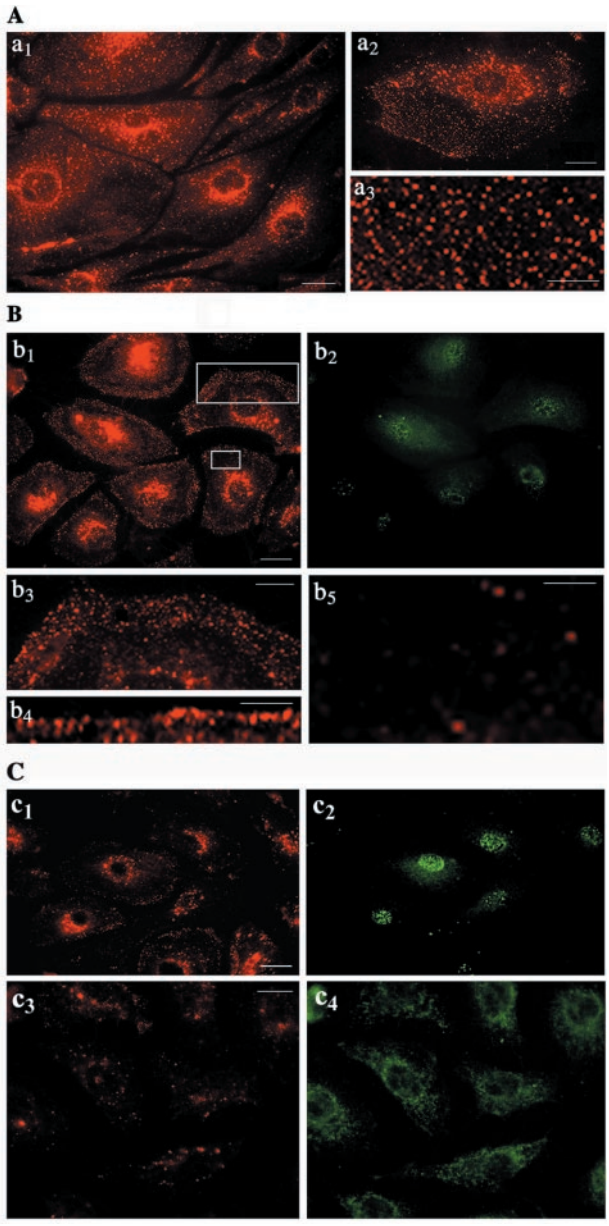

Figure 6. Expression of wt-intersectin inhibits caveolae internalization. (A) In control cells subjected to biotinylation of cell surface proteins and internalization assay, fluorescent staining with neutrAvidin Texas Red indicates a strong punctate pattern throughout the cytosol a_1 (see inset a_3 for a higher magnification) with accumulation in the perinuclear area. Inset a_2 shows an enlarged EC subjected to the internalization assay. Note the relatively limited labeling at the cell surface because of the internalization. (B) ECs transiently transfected with myc-tagged wt-intersectin were selected based on their resistance to blasticidin and subjected to the internalization assay; anti-myc mAb followed by anti-mouse IgG FITC were used to visualize the transfected cells (b_2). NeutrAvidin Texas Red revealed a generalized prominent fine punctate cell surface staining (b_1 and b_4). A strong punctate, belt-like staining was often seen at the plasma membrane (b_3) below which was a region of low density of puncta (b_5). Panels b_3 and b_5 are enlarged versions of the boxed regions in b_1. (C) Effects of ΔSH3A and DN-intersectin on biotinylated cell surface protein internalization. ECs expressing ΔSH3A (c_1) or DN-intersectin (c_3) were subjected to the biotin internalization assay. NeutrAvidin Texas Red showed a limited staining in both cases. Anti-myc mAb followed by anti-mouse IgG FITC were used to visualize the transfected cells (c_2, c_4). Bars, (a_1, a_2, b_1, c_1, and c_3) 10 μm, (a_3 and b_3) 10 μm, and (b_4 and b_5) 7.5 μm.

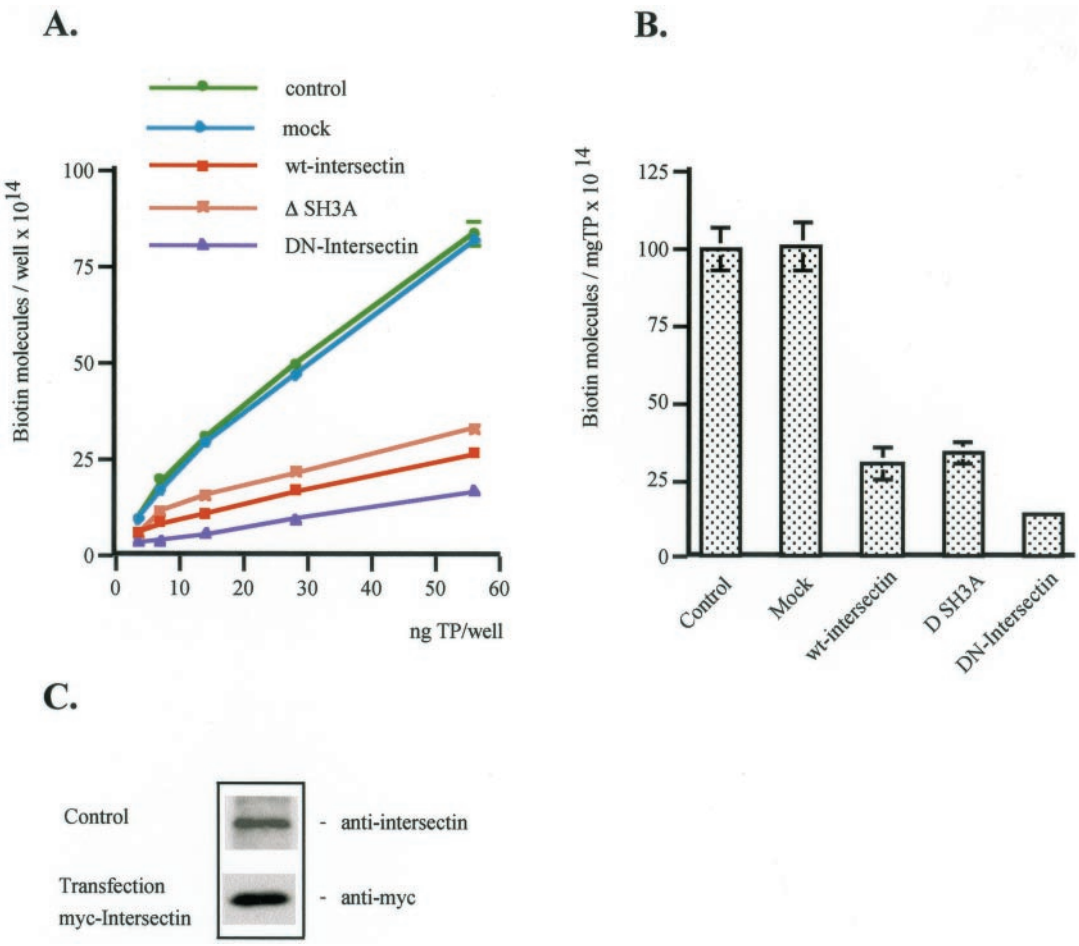

Figure 7. Effects of wt-intersectin overexpression on caveolae-mediated uptake. (A) The number of biotin molecules present in the EC lysates containing the internalized biotinylated cell surface proteins in control, mock, wt-intersectin ΔSH3A, or DN-intersectin transfected cells was determined by ELISA in 4–5 experiments. Ordinate: number of biotin molecules per well; abscissa: ng total protein (TP) per well. (B) Degree of inhibition of caveolae-mediated uptake in transfected cells compared with control. Bars, ±SD. (C) Cultured ECs were transiently transfected with the DNA construct encoding myc tagged wt-intersectin. After protein expression, cells were lysed and processed along with an aliquot of untransfected ECs lysate (control) for Western blots with anti-intersectin pAb or anti-myc mAb, respectively.

plasma membrane patches bearing attached caveolae (Stan *et al.*, 1997) were incubated with EC cytosol, 1 mM GTP, and an ATP-regenerating system, conditions that promote caveolae fission (Schnitzer *et al.*, 1996). Caveolae fission was monitored biochemically by sucrose density centrifugation and morphologically by immunogold labeling and negative staining EM. The released caveolae were detected by SDS-PAGE and immunoblotting with anti-caveolin pAb in fractions 5–11 of sucrose gradients as low-density membranes that were caveolin enriched (Figure 4A). EM-negative staining and immunogold labeling revealed in the same fractions a homogeneous population of vesicles, 70–90 nm in diameter (Figure 4Ba) that were heavily labeled by 10 nm gold conjugated anti-caveolin pAb (Figure 4Bb). This anti-caveolin antibody has been characterized and used previously for immunoisolation of caveolae on magnetic beads (Stan *et al.*, 1997). To address the role of intersectin in caveolae release, plasma membrane patches depleted of intersectin by high salt were incubated with cytosol that was intersectin-immunodepleted by specific antibodies against intersectin. This was necessary because intersectin is present in both membrane-associated (Okamoto *et al.*, 1999) and soluble pools (Tong *et al.*, 2000). The cytosolic fraction, intersectin-depleted, maintained its dynamin immunoreactivity as assessed by Western blotting (our unpublished results). This is not surprising considering that intersectin-dynamin interaction was not detected by cross-linking in the endothelial cytosolic fraction. On depletion of intersectin by this means, the plasma membrane-attached caveolae failed to undergo fission; i.e., caveolin was not detected in the light fractions of sucrose gradients (Figure 4C). Similar results were obtained when plasma membrane patches were incubated with GTP and ATP in the absence of cytosol. These results establish that intersectin is required for caveolae release from the plasmalemma. Immunoblot signals for caveolin detected in equivalent aliquots from the light membrane fractions of sucrose gradients, the starting material (PM patches), and the repelleted silica-coated membranes were quantified densitometrically (Figure 4D).

Expression of wt-Intersectin Inhibits Caveolae Internalization

We addressed using a biotin internalization assay (Zurzolo *et al.*, 1994) the effects of overexpressing wt-intersectin on

Figure 8. Electron micrographs of ECs overexpressing wt-intersectin. Micrographs show partial views of cultured ECs overexpressing wt-intersectin. The cells maintain a large population of caveolae open to the apical (A) or basolateral (B) fronts of the cells or apparently free in the cytosol (arrows). The majority of caveolae profiles are part of large clusters of interconnected caveolae, "grape-like" structures or with unusual shapes, accumulated at the cell periphery. Insets in A illustrate additional "grape-like" (a_1, a_2) or unusually shaped (a_3), caveolae clusters. Note the caveolar profiles displaying staining-dense rings (arrowheads). Bars, 50 nm.

caveolae internalization in ECs. It is well documented that ECs possess a large population of caveolae and that transcytosis mediated by caveolae is a major function of the endothelium (Simionescu and Simionescu, 1991; Palade *et al.*, 1997). The transport is rapid (9–30 s) and a vesicle acts as a shuttle between the luminal and abluminal front of the cell (Boyles *et al.*, 1981; Tuma and Hubbard, 2003). Furthermore, the population of CCVs in ECs is relatively small (Palade *et al.*, 1979) and they have a minor contribution to the internalization process (Simionescu and Simionescu, 1991). First, to validate the use of biotinylated cell surface proteins as probes for caveolar uptake, a double internalization assay was carried out using both, a cleavable biotin reagent and cholera toxin (CT) subunit B. For morphological survey by fluorescence, we used CT-FITC, whereas the biotinylated toxin was used for quantitative assessment of internalization by ELISA. CT is widely accepted as a marker for caveolae-mediated uptake (Schnitzer *et al.*, 1996; Tran *et al.*, 1987). CT binds specifically the ganglioside GM1 that is concentrated in caveolae (Parton *et al.*, 1994) and is largely excluded from clathrin-positive regions of the plasma membrane (Nichols, 2003). The double fluorescent labeling analysis of the uptake showed a similar staining pattern for both biotinylated cell surface proteins and CT-FITC (Figure 5, a and b). The internalized biotinylated proteins were detected with neutrAvidin Texas Red. We observed fine puncta at the cell surface and scattered all over the cytoplasm with a propensity to accumulate in the perinuclear region. The overlapped image (Figure 5c, and inset c1) indicated a high degree of colocalization of both probes. Inset b1 shows binding of CT-FITC to the EC surface at 4°C. The quantitative assessment of internalization of biotinylated cell surface proteins and CT-biotin by ELISA indicated that both probes were internalized to the same magnitude (Figure 5e). We detected $57 \pm 3.1 \times 10^{14}$ biotin molecules/mg total protein when biotinylated cell surface proteins were internalized, and $48.5 \pm 2.7 \times 10^{14}$ biotin molecules/mg total protein when CT-biotin was used; these results indicate that ~85% of the internalization process is dependent on caveolae. Similar results were obtained in control experiments where cultured ECs first were depleted of K^+ (Larkin *et al.*, 1983) to inhibit the clathrin-mediated pathway before the biotin internalization assay. A punctate staining pattern (Figure 5d) and a similar number of biotin molecules found in the lysates of K^+-depleted ECs (Figure 5e) support findings on the major contribution of endothelial caveolae in the internalization process. The punctate pattern overlapped a slight diffuse staining explained by the fact that hypotonically shocked cells have, as seen in Figure 5d and as previously reported (Larkin *et al.*, 1983), a more condensed cytosol and a smaller nucleus than control cells. Thus taken together, our morphological and quantitative data demonstrate that internalization of biotinylated cell surface proteins in ECs is mediated primarily by caveolae.

To evaluate the effects of intersectin overexpression on caveolae internalization, control and transfected cells were exposed to a cleavable biotin reagent and processed for morphological and biochemical analyses. In controls (Figure 6A), the fluorescent staining indicated an extensive fine punctate pattern throughout the cell (a_1, a_3) with some accumulation in the perinuclear region (a_1, a_2). In cells transfected with myc-tagged wt-intersectin (Figure 6B), the staining was reduced; interestingly, biotin was detected in punctate structures marginated at the cell periphery (b_1, b_4) or accumulated in a fluorescent punctate belt-like structure under the plasma membrane (b_3). No staining or low density of puncta was observed beneath these vesicular structures

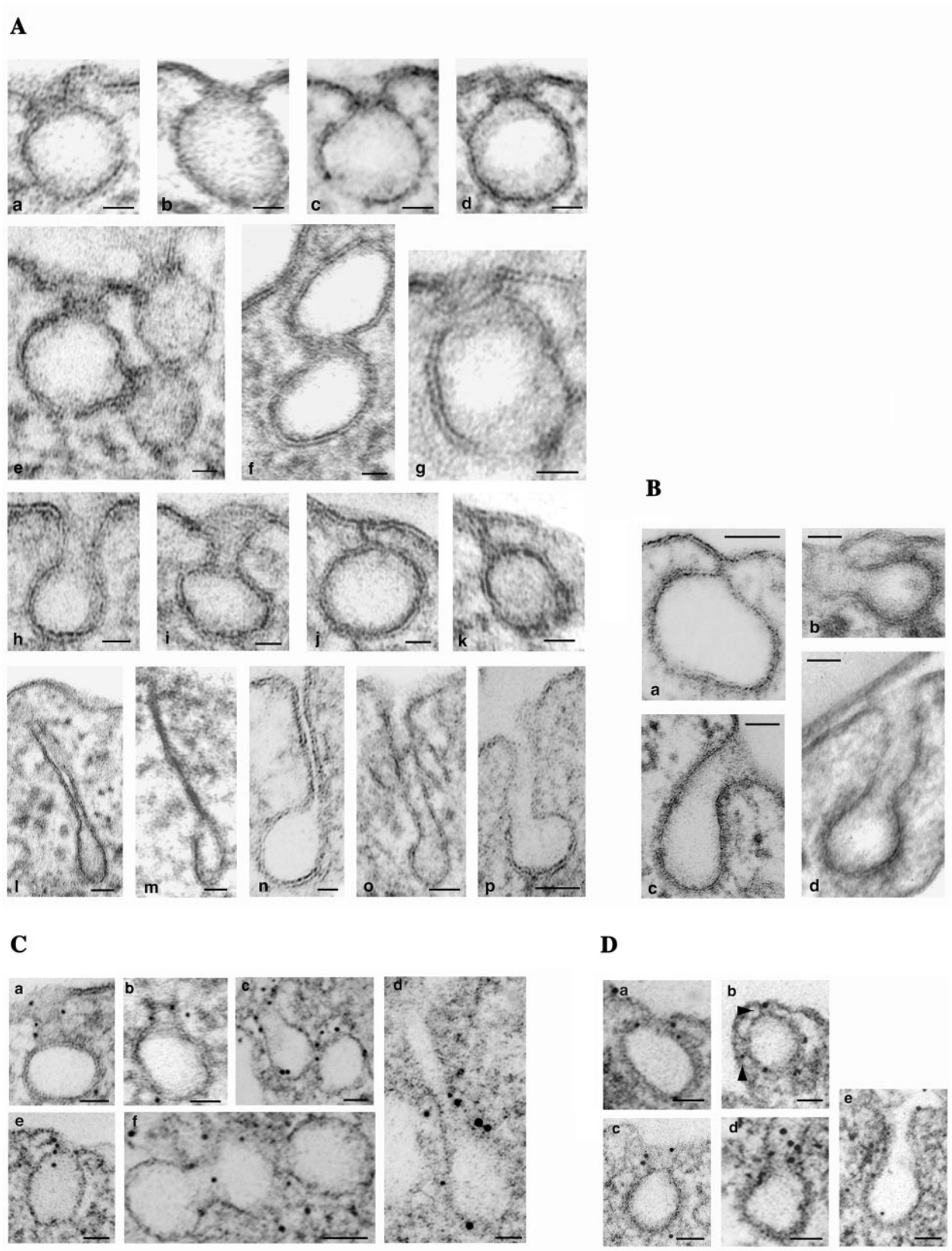

Figure 9.

marginated at the cell periphery (b_5). These findings suggest accumulation of caveolae that are unable to move through the cell cortex into the cytosol. Moreover, the resistance of biotin to glutathione, a membrane impermeant reducing agent (Bretscher and Lutter, 1988), indicated the lack of connection between these marginated vesicular structures and the cell surface. The transfected cells in these experiments were detected with anti-myc mAb (b_2, c_2, c_4). We have also examined if the truncated form of intersectin deleted of its SH3A domain, (ΔSH3A), or the dominant negative construct, (DN-intersectin), containing only the five SH3 domains (Fumitoshi and Yamaguchi, 2002), inhibited caveolae-mediated uptake. Among intersectin's five SH3 domains, the SH3A has the highest binding affinity for dynamin (Yamabhay *et al.,* 1998). We found that the fluorescent staining was extremely limited in both ΔSH3A and DN-intersectin expressing cells, suggesting inhibition of caveolae-mediated internalization of biotinylated cell surface proteins (c_1, c_3).

To evaluate quantitatively the effects of wt-intersectin overexpression, we estimated by ELISA the number of biotin molecules in control and transfected EC lysates. ELISA was applied on transiently transfected cells that had been selected based on their blasticidin resistance. In all lysates prepared from transfected cells, the number of biotin molecules was markedly reduced (Figure 7A). The inhibition of uptake was 68.4% by reference to control (Figure 7B). Thus, as suggested by fluorescence, accumulation of caveolae unable to move through the cell cortex into the cytosol accounts for the marked decrease in the uptake of biotinylated proteins in cells overexpressing wt-intersectin. In cells overexpressing ΔSH3A or DN-intersectin, we observed using biochemical measurements a 65% and >80% reduction of caveolae release, respectively (Figure 7, A and B). This finding is in agreement with our immunofluorescence data, further establishing the crucial role of intersectin in caveolae fission. Expression of wt-intersectin in transfected cells, monitored by Western blotting with anti-myc mAb, indicated that the 140-kDa protein corresponding to intersectin was threefold greater than the endogenous level (Figure 7C).

To better understand the effects of intersectin overexpression in ECs, we performed a detailed morphological analysis by EM. Transfected cells accumulated large clusters of caveolae at the cell periphery (Figure 8, A and B) many with no apparent connection to the cell surface. Serial sectioning applied on transfected cells confirmed that majority of these structures had no communication to the cell surface (our unpublished results). On the basis of these findings, we assumed that some of the caveolae detached from the plasmalemma formed either discrete vesicular carriers (Figure 8A, arrows) or caveolae clusters by caveolae fusion, thereby sequestering the biotinylated proteins. Moreover, their accumulation at the cell periphery suggested their failure to be released through the cell cortex and their impaired movement into the cytosol. Extensive morphometric analysis of control and transfected cells indicated that there was no significant change in the total number of caveolae open on either front of the cell or apparently free in the cytosol. However, in transfected cells, the majority of caveolae open o the cell surface or apparently free in the cytosol were part of large "grape-like" clusters (Figure 8A and insets a_1, a_2) or had uncommon shapes (Figure 8A, a_3) formed by 7–10 or more interconnected caveolae. In transfected cells, 69% of caveolae in the cytosol were clustered and marginated. Similar clustering occurred when the caveolae were open apically (68%) or basolaterally (74%). In control cells, caveolae clusters (usually 4–6 interconnected caveolae) comprised an average of 27% caveolae open to the cell surface and ~40% caveolae in the cytosol. Besides clustering, we observed: 1) caveolae open to the cell surface displaying narrow necks surrounded by dense-stained rings (Figures 8B, arrowheads, and 9A, a–d), which were frequently associated with the constricted region of two adjacent caveolae (Figure 9A, e and f), and in favorable sections almost complete collars encircling the caveolae neck (Figure 9Ag), 2) caveolae with elongated necks (Figure 9A, h and i), 3) closed caveolae tethered to the plasmalemma (Figure 9A, j and k), and 4) caveolae with extremely long necks (Figure 9A, l–p), which in favorable sections were connected to the plasmalemma (Figure 9, m–p). Despite of the reduced number of clathrin-coated pits (CCPs) in ECs, we observed that the CCPs in intersectin-overexpressing ECs also remained attached to the plasmalemma (Figure 9Ba) and that there were CCPs with elongated necks (Figure 9B, b–d), similar to the morphological intermediates produced by dynamin GTPase domain mutants in tTA-HeLa cells (Damke *et al.,* 2001). EM immunogold study indicated dynamin immunoreactivity at the level of elongated necks of invaginated caveolae (Figure 9C, a–e) and CCPs (Figure 9D, a–e) as well as at constriction sites between adjacent caveolae in caveolar clusters (Figure 9C, c and f).

Figure 9 (facing page). Gallery of representative caveolae profiles (A) and CCPs (B) and dynamin immunoreactivity (C and D) in ECs overexpressing wt-intersectin. Micrographs in A show highly magnified staining-dense rings surrounding the necks of caveolae open to the cell surface (a–d), constricted region between two adjoining caveolae (e and f), caveolae with elongated necks (h and i), caveolae attached to the plasmalemma and unable to move into the cytosol (j and k), and caveolae with extremely long necks (l–p). The micrograph in panel g shows in a favorable section an almost complete ring encircling a caveolae neck. A caveolae neck of ~70 nm length (the vesicle diameter) was considered as elongated neck. The figures shown in these panels were not seen in normal cells. Bars, (a–k and n) 20 nm, (l, m, o, and p) 50 nm. (B) CCV attached to the plasmalemma, just before release into the cytosol (a) and CCPs displaying elongated (b and c) or long necks (d). Bars, 50 nm. (C) Representative electron micrographs show dynamin immunoreactivity at the level of elongated caveolar necks (a–c), constricted region between adjacent caveolae (c and f), and staining-dense ring encircling a caveolae neck (e). A long caveolae neck immunoreactive to dynamin antibody is shown in d. Bars, (a, b, d, and e) 25 nm; (c and f) 35 nm. (D) Dynamin immunoreactivity is associated with a staining-dense ring surrounding the neck of a deep pit (a), elongated pits (c–e), or a CCP displaying two necks (d, arrowheads). Bars, 50 nm.

DISCUSSION

Transcytosis mediated by caveolae is a major transport pathway in ECs. Although caveolae are the primary vesicle carriers responsible for transcytosis in endothelial cells (Simionescu and Simionescu, 1991), the mechanisms of their fission from the plasma membrane remain unclear. Previous studies (Schnitzer *et al.,* 1995; Apodaca *et al.,* 1996; Oh *et al.,* 1998; Predescu *et al.,* 2001) as well as this one strongly suggest that common molecular mechanisms that underlie a variety of vesicle-mediated transport steps from yeast vacuole to the mammalian nerve terminal operate also in transcytosis. In the present study, we have addressed the role of intersectin in the caveolae internalization. We demonstrated by several biochemical procedures such as coimmunoprecipitation, velocity sedimentation on glycerol gradients, and

cross-linking the strong association of intersectin with dynamin and SNAP-23. The cross-linking experiments using DST, a membrane-permeant cross-linker applied to intact cultured ECs, showed that the three proteins formed a membrane-associated complex, suggesting that these interactions that may be critical for caveolae release occur at the membrane level. We also observed by immunofluorescence the extensive colocalization of intersectin with both caveolin, the generally accepted caveolar marker (Rothberg *et al.*, 1992) and dynamin, the GTPase required for caveolae fission. EM immunogold labeling showed the association of intersectin with caveolae in greater detail such as its preferential localization at the neck region of caveolae. Significantly, both intersectin and dynamin were also localized at constriction sites between two adjoining caveolae and with caveolae apparently free in the cytosol after their detachment from the plasmalemma. These findings support a functional role of intersectin-dynamin interaction in the mechanism of caveolae fission. Moreover, the association of intersectin with other membranous organelles, the Golgi and CCVs, also suggests its involvement in different vesicular pathways.

Quantitative analysis of internalization by caveolae using biotinylated cell surface proteins or CT-biotin as probes demonstrated that caveolae contributed to greater than 85% of the uptake process in ECs. In support of this, K^+-depletion used to inhibit internalization by CCVs did not significantly affect the internalization of the biotinylated cell surface proteins. Thus, caveolae-mediated uptake is by far the dominant mechanism of internalization in ECs.

In the present study, we have established the functional role of intersectin in the mechanism of caveolae fission using both a cell-free system depleted of intersectin and intact cultured ECs overexpressing DN-intersectin. Intersectin depletion prevented the GTP-dependent release of caveolae from plasma membrane sheets, a critical step in the formation of caveolae-derived vesicular carriers (Schnitzer *et al.*, 1996). These findings show that the GTP-dependent caveolae release requires intersectin. Although dynamin was present in this system, it alone was not sufficient to induce caveolae fission. A DN-intersectin consisting only of the SH3 domains markedly inhibited caveolae internalization consistent with a crucial role of intersectin in caveolae fission.

We also carried out studies to assess the effects of wt-intersectin overexpression in ECs. The biotin internalization assay used in cultured ECs overexpressing wt-intersectin indicated by light and EM impairment in membrane fission and the failure of caveolae to move through the cell cortex into the cytosol. Caveolae-mediated uptake was reduced 68% compared with controls. Detection of glutathione-resistant biotin in the marginated caveolae structures in the cell cortex indicated their lack of communication with the cell surface; thus, the overexpression of wt-intersectin had apparently sealed the marginated caveolae after their fission from the plasma membrane. Interestingly, expression of the ΔSH3A construct in cultured ECs resulted in significant

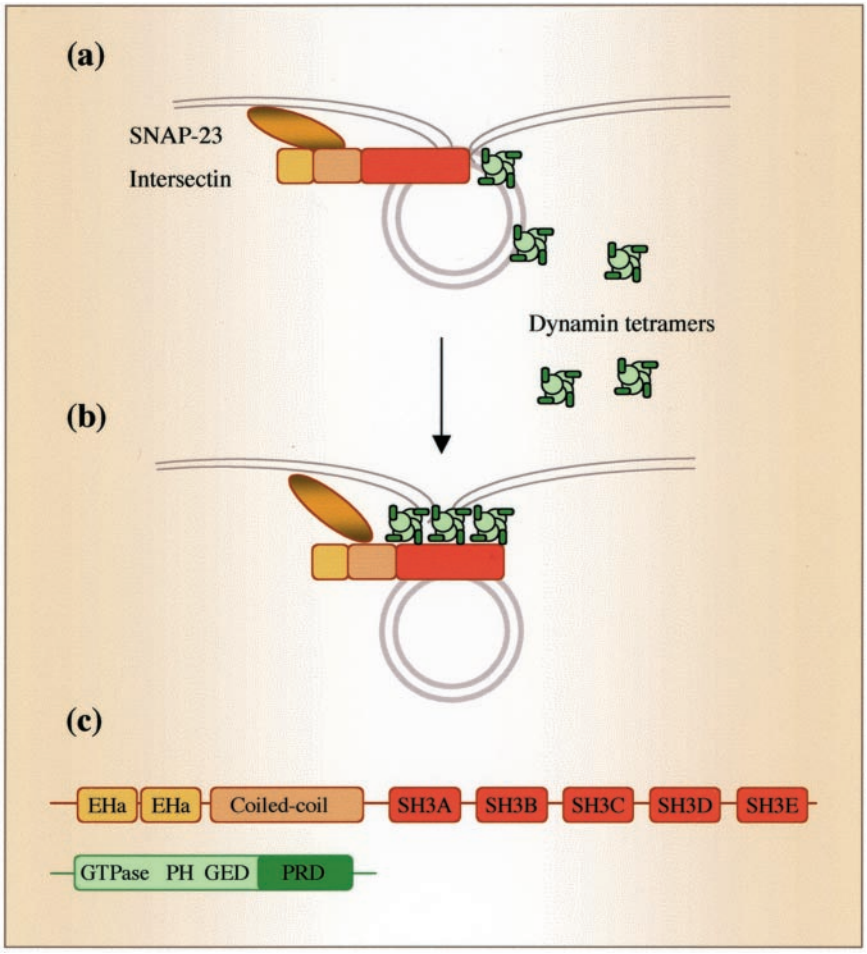

Figure 10. Role of intersectin-dynamin interaction in caveolae dynamics. In this model, the intersectin-dynamin interaction plays a central role in caveolae fission. Both intersectin and dynamin are preferentially associated with the caveolae neck (a). Intersectin binds and clusters dynamin in the proximity of the plasma membrane generating a high local dynamin concentration required for ring formation around caveolar necks. Dynamin bound to intersectin is functionally impaired and fission is restrained (b). Domain structures of intersectin and dynamin (c). Intersectin binds the PRD domain of dynamin via a subset of its SH3 domains (SH3A, SH3C, and SH3E).

inhibition of caveolae internalization as assessed morphologically and biochemically. This finding suggests an essential involvement of the SH3A domain, an inhibitor of endocytosis (Simpson *et al.,* 1999) and a dynamin interacting-module (Yamabhay *et al.,* 1998), in regulating intersectin function. By EM, we observed that the ECs overexpressing wt-intersectin displayed a range of morphological changes (i.e., extensive caveolae clustering, large caveolae clusters marginated at the cell periphery, and pleiomorphic caveolar necks). These changes were likely the consequence of simultaneous overexpression of intersectin's five protein-protein interaction modules involved in regulating endocytic events. The extensive caveolae clustering, and as a result impaired internalization and movement of caveolae, is a unique finding. Clustering is a process characteristic for caveolae-derived vesicular carriers with a high propensity to fuse and form interconnected "grape-like" structures (Simionescu and Simionescu, 1991; Predescu *et al.,* 2001). We observed the extensive accumulation at the cell periphery of large caveolae clusters in which caveolae are in close contact, fuse to each other, and lose their normal shape and caveolae with modified necks. Comparable pleiomorphic modifications of necks of CCPs were also seen with intersectin overexpression, suggesting similarities in the scission steps of caveolae and CCPs. Thus, the findings suggest that intersectin is a key protein required for fission of both caveolae and CCPs in ECs.

Intersectin binds via three of its five SH3 domains to the proline-rich COOH-terminus domain of dynamin (Yamabhay *et al.,* 1998; Okamoto *et al.,* 1999). Recent studies showed that interactions of dynamin with SH3-domain–containing proteins such as amphiphysin-2 (Owen *et al.,* 1998; Takei *et al.,* 1999) and intersectin (Simpson *et al.,* 1999) are important in regulating the formation of CCVs. In the present study, intersectin overexpression did not interfere with dynamin recruitment to the neck region of caveolae or CCPs; that is, we observed dynamin immunogold labeling of the elongated caveolar necks and invaginations of CCPs in the ECs overexpressing intersectin. Intersectin is a strategically located peripheral membrane-associated protein (Okamoto *et al.,* 1999) that is able to bind and cluster dynamin (dimers and tetramers in its native state; Muhlberg *et al.,* 1997). Thus, the present data suggest a model in which intersectin recruits dynamin in the proximity of the plasma membrane to facilitate its interactions with membrane lipids and generate a high local concentration of dynamin required for the collar formation at the neck (Figure 10). However, dynamin remains functionally impaired and fission does not occur as long as dynamin is bound to intersectin. Intersectin may also act in concert with other proteins and lipids to regulate dynamin function (O'Brian *et al.,* 2001; McPherson, 2002) and thereby different steps in caveolae internalization.

Dynamin is believed to function by GTP-triggered self-assembly into a helical collar around the neck of invaginated pits or caveolae, followed by coordinated GTP-hydrolysis and release of vesicles from plasmalemma (Takei *et al.,* 1995; Oh *et al.,* 1998; Schmid *et al.,* 1998). Although the physiological significance of dynamin collars, thought to be dynamin associated with other factors (Sever *et al.,* 2000), seems to be indisputable, they have not previously been observed to be associated with caveolae. In the present study, we detected in intact ECs not transfected with dynamin mutants, staining-dense rings encircling short caveolar necks similar to the collars described around necks of endocytic vesicles in nerve terminals of *shibire* flies (Takei *et al.,* 1995). We showed that overexpression of intersectin stabilized the caveolar necks and collars, thus enabling their detection by EM. Based on similarities between the effects of intersectin overexpression in ECs and expression of dynamin GTPase domain mutants on CCV formation (Damke *et al.,* 2001), it is tempting to speculate that intersectin regulates dynamin's enzymatic activity and self-assembly. Thus, intersectin may hold in abeyance the dynamin multimers and other components of the caveolae internalization machinery consistent with the scaffolding function of intersectin's SH3 domains.

The role of actin in caveolae internalization (Pelkmans and Helenius, 2002; Pelkmans *et al.,* 2002) as regulated by intersectin also needs to be considered. Intersectins interact through a subset of their SH3 domains with N-WASP, which regulates actin polymerization by stimulating actin-nucleating activity of Arp2/3 complex (Hussain *et al.,* 2001; McPherson, 2002). Our overlay studies using the SH3A domain of intersectin showed WASP to be an intersectin-interacting protein in ECs (our unpublished results). Thus, it is possible that overexpression of wt-intersectin interfered with local actin organization and thereby may have also contributed to inhibiting the internalization of caveolae.

ACKNOWLEDGMENTS

We are grateful to Dr. T. Südhof for generously providing anti-intersectin antibodies and to Dr. B.B. Kay, for cDNA encoding *Xenopus laevis* intersectin. We especially thank Dr. G.E. Palade for helpful discussions and advice. We also thank Nicki Watson for technical assistance with electron microscopy. This work was supported by PO1 HL60678 (A.B.M.). Part of this work was supported by National Institutes of Health Grant HL 17080 to G.E.P. at UCSD.

REFERENCES

Adams, A., Thorn, J.M., Yamabhai, M., Kay, B.K., and O'Brian, J.P. (2000). Intersectin, an adaptor protein involved in clathrin-mediated endocytosis activates mitogenic signaling pathways. J. Biol. Chem. *275,* 27414–27420.

Anderson, E., Hellman, L., Gullberg, U., and Olsson, I. (1998). The role of the propeptide for processing and sorting of human myeloperoxidase. J. Biol. Chem. *273,* 4747–4753.

Apodaca, G., Cardone, M.H., Whiteheart, S.W., DasGupta, B.R., and Mostov, K.E. (1996). Reconstitution of transcytosis in SLO-permeabilized MDCK cells: existence of an NSF-dependent fusion mechanism with the apical surface of MDCK cells. EMBO J. *15*(7), 1471–1481.

Boyles, J., L'Hernault, N., Laks, H., and Palade, G.E. (1981). Evidence for a vesicular shuttle in heart capillaries. J. Cell Biol. *91,* 418a.

Bretscher, M.S., and Lutter, R. (1988). A new method for detecting endocytosed proteins. EMBO J. *7,* 4087–4092.

Damke, H., Binns, D.D., Ueda, H., Schmid, S.L., and Baba, T. (2001). Dynamin GTPase domain mutants block endocytic vesicle formation at morphologically distinct stages. Mol. Biol. Cell *12,* 2578–2589.

Fumitoshi, I., and Yamaguchi, Y., (2002). EphB receptors regulate dendritic spine development via intersectin, Cdc42 and N-WASP. Nat. Neurosci. *5,* 117–118.

Guipponi, M., Scott, H.S., Chen, H., Schebesta, A., Rossier, C., and Antonarakis, S.E. (1998). Two isoforms of a human intersectin (ITSN) protein are produced by brain-specific alternative splicing in a stop codon. Genomics *53,* 369–376.

Henley, J.R., Krueger, E.W.A., Oswald, B.J., and McNiven, M.A. (1998). Dynamin-mediated internalization of caveolae. J. Cell Biol. *141,* 85–99.

Hussain, N.K. *et al.* (2001). Endocytic protein intersectin-l regulates actin assembly via Cdc42 and N-WASP. Nat. Cell Biol. *3,* 927–932.

Hussain, N.K., Yamabhai, M., Ramjaun, A.R., Guy, A.M., Baranes, D., O'Bryan, J.P., Der, C.J., Kay, B.K., and McPherson, P.S. (1999). Splice variants of intersectin are components of the endocytic machinery in neurons and nonneuronal cells. J. Biol. Chem. *274,* 15671–15677.

Larkin, M.J., Brown, M.S., Goldstein, J.L., and Anderson, R.G.W. (1983). Depletion of intracellular potassium arrests coated pit formation and receptor-mediated endocytosis in fibroblasts. Cell *33,* 273–285.

Lencer, W.I., Delp, C., Neutra, M.R., and Madara, J.L. (1992). Mechanism of cholera toxin action on a polarized human intestinal epithelial cell line: role of vesicular traffic. J. Cell Biol. *117*, 1197–1209.

McPherson, P.S. (2002). The endocytic machinery at an interface with the actin cytoskeleton: a dynamic, hip intersection. Trends Cell Biol. *12,* 312–315.

Minshall, R.D., Tiruppathi, C., Vogel, S.M., Niles, W.D., Hamm, H.E., and Malik, A.B. (2000). Endothelial cell-surface gp60 activates vesicle formation and trafficking via G(i)-coupled Src kinase signaling pathway. J. Cell Biol. *150,* 1057–1070.

Muhlberg, A.B., Warnock, D.E., and Schmid, S.L. (1997). Domain structure and intramolecular regulation of dynamin GTPase. EMBO J. *16,* 6676–6683.

Nichols, B.J. (2003). GM1-containing lipid rafts are depleted within clathrin-coated pits. Curr. Biol. *13,* 686–690.

Niles, W.D., and Malik, A.B. (1999). Endocytosis and exocytosis events regulate vesicle traffic in endothelial cells. J. Membr. Biol. *167,* 85–101.

O'Brian, J.P., Mohney, R.P., and Oldham, C.E. (2001). Mitogenesis and endocytosis: What's at the INTERSECTION? Oncogene *20,* 6300–6308.

Oh, P., McIntosh, D.P., and Schnitzer, J.E. (1998). Dynamin at the neck of caveolae mediates their budding to form transport vesicles by GTP-driven fission from the plasma membrane of endothelium. J. Cell Biol. *141,* 101–114.

Okamoto, M., Schoch, S., and Südhof, T.C. (1999). EHSH1/Intersectin, a protein that contains EH and SH3 domains and binds to dynamin and SNAP-23. J. Biol. Chem. *274,* 18446–18454.

Owen, D.J., Wigge, P., Vallis, Y., Moore, J.D., Evans, P.R., and McMahon, H.T. (1998). Crystal structure of the amphiphysin-2 SH3 domain and its role in the prevention of dynamin ring formation. EMBO J. *17,* 5273–5285.

Palade, G.E., Predescu, D., Predescu, S., and Stan, R.V. (1997). Malpighi's heritage three centuries later. Recent Advances in Microscopy of Cells, Tissues and Organs, 9–19.

Palade, G.E., Simionescu, M., and Simionescu, N. (1979). Structural aspects of the permeability of the microvascular endothelium. Acta Physiol. Scand. Suppl. *463*, 11–32.

Parton, R.G., Joggerst, B., and Simons, K. (1994). Ultrastructural organization of gangliosides; GM1 is concentrated in caveolae. J. Histochem. Cytochem. *42,* 155–166.

Pathak, R.K., and Anderson, R.G.W. (1989). Use of dinitrophenol-IgG conjugates to detect sparse antigens by immunogold labeling. J. Histochem. Cytochem. *37,* 69–74.

Pelkmans, L., and Helenius, A. (2002). Endocytosis via caveolae. Traffic *3,* 311–320.

Pelkmans, L., Pluntener, D., and Helenius, A. (2002). Local actin polymerization and dynamin-induced internalization of caveolae. Science *296,* 535–538.

Predescu, D., Ihida, K., Predescu, S., and Palade, G.E. (1995). The vascular distribution of the platelet-activating factor receptor. Eur. J. Cell Biol. *69,* 86–98.

Predescu, S., Predescu, D., and Palade, G.E. (1997a). Plasmalemmal vesicles function as transcytotic carriers for small proteins in the continuous endothelium. Am. J. Physiol. *272,* H937–H949.

Predescu, S., Predescu, D., and Palade, G.E. (1997b). Endothelial transport machinery—a supramolecular protein-lipid complex. Mol. Biol. Cell Suppl. *8*, 232a.

Predescu, S., Predescu, D., and Palade, G.E. (2001). Endothelial transcytotic machinery involves supramolecular protein-lipid complexes. Mol. Biol. Cell *12,* 1019–1033.

Pucharcos, C., Estivill, X., and de la Luna, S. (2000). Intersectin 2, a multimodular protein involved in clathrin-mediated endocytosis. FEBS Lett. *478,* 43–51.

Quagliarello, V.J., Ma, A., Stukenbrok, H., and Palade, G.E. (1991). Ultrastructural localization of albumin transport across the cerebral microvasculature during experimental meningitis. J. Exp. Med. *174,* 657–672.

Roos, J., and Kelly, R.B. (1998). Dap160, a neural-specific Eps 15 homology and multiple SH3 domain-containing protein that interacts with *Drosophila* dynamin. J. Biol. Chem. *273,* 19108–19119.

Rothberg, K.G., Heuser, J.E., Donzell, W.C., Ying, Y.S., Glenney, J.R., and Anderson, R.G. (1992). Caveolin, a protein component of caveolae membrane coats. Cell. *68*, 673–682.

Savage, M.D., Mattson, G., Desai, S., Nielander, G.W., Morgensen, S., and Couklin, E.J. (1992). Avidin-Biotin Chemistry: A Handbook. Rockford, IL: Pierce, 195–215.

Schmid, S.L., McNiven, M.A., and DeCamilli, P. (1998). Dynamin and its partners: a progress report. Curr. Opin. Cell Biol. *10*, 504–512.

Schnitzer, J.E., Liu, J., and Oh, P. (1995). Endothelial caveolae have the molecular transport machinery for vesicle budding, docking, and fusion, including VAMP, NSF, SNAP, annexins and GTPases. J. Biol. Chem. *270,* 14399–14404.

Schnitzer, J.E., Oh, P., and McIntosh, D.P. (1996). Role of GTP hydrolysis in fission of caveolae directly from the plasma membrane. Science *274,* 239–242.

Sengar, A.S., Wang, W., Bishay, J., Cohen, S., Schebesta, A., Rossier, C., and Antonarakis, S.E. (1999). The EH and SH3 domain Ese proteins regulate endocytosis by linking to dynamin and Eps 15. EMBO J. *18,* 1159–1171.

Sever, S., Damke, S., and Schmid, S.L. (2000). Garrotes, springs, ratchets, and whips: Putting dynamin models to the test. Traffic *1,* 385–392.

Simionescu, M., and Simionescu, N. (1984). Ultrastructure of the microvascular wall: functional correlations. In: Handbook of Physiology—The Cardiovascular System. In: eds. E.M. Renkin and C.C. Michel, Microcirculation, vol. IV, pt. I, chapt. 3, Bethesda, MD: American Physiological Society, 78–86.

Simionescu, M., and Simionescu, N. (1991). Endothelial transcytosis of macromolecules: transcytosis and endocytosis. Cell Biol. Rev. *25,* 1–80.

Simpson, F., Hussain, N.K., Qualmann, B., Kelly, R.B., Kay, B.K., McPherson, P.S., and Schmid, S.L. (1999). SH3-domain-containing proteins function at distinct steps in clathrin-coated vesicle formation. Nat. Cell Biol. *1,* 119–124.

Slot, J.W., and Geuze, H.J. (1985). A new method of preparing gold probes for multiple labeling cytochemistry. Eur. J. Cell Biol. *38,* 87–93.

Smith, R.J., Capaldi, R.A., Muchmore, D., and Dahlquist, F. (1978). Cross-linking of ubiquinone cytocrome c reductase (complex III) with periodate-cleavable bifunctional reagents. Biochemistry *17,* 3719–3723.

Stan, R.V., Roberts, W.G., Predescu, D., Ihida, K., Saucan, L., Ghitescu, L., and Palade, G.E. (1997). Immunoisolation and partial characterization of endothelial plasmalemmal vesicles (caveolae). Mol. Biol. Cell *8,* 595–605.

Takei, K., McPherson, P.S., Schmid, S.L., and DeCamilli, P. (1995). Tubular membrane invaginations coated by dynamin rings are induced by GTP-γS in nerve terminals. Nature *374,* 186–189.

Takei, K., Slepnev, V.I., Haucke, V., and DeCamilli, P. (1999). Functional partnership between amphiphysin and dynamin in clathrin-mediated endocytosis. Nat. Cell Biol. *1,* 33–39.

Tong, X.K. *et al.* (2000). The endocytic protein intersectin is a major binding partner for the Ras exchange factor mSos1 in rat brain. EMBO J. *19,* 1263–1271.

Tran, D., Carpentier, J.L., Sawano, F., Gorden, P., and Orci, L. (1987). Ligands internalized through coated or noncoated invaginations follow a common intracellular pathway. Proc. Natl. Acad. Sci. USA *84,* 7957–61.

Tuma, P., and Hubbard, A.L. (2003). Transcytosis: crossing cellular barriers. Physiol. Rev. *83,* 871–932.

Yamabhay, M., Hoffman, N.G., Hardison, N.L., McPherson, P.S., Castagnoli, L., Cesareni, G., and Kay, B.K. (1998). Intersectin, a novel adaptor protein with two Eps15 homology and five Src homology 3 domains. J. Biol. Chem. *273,* 31401–31407.

Zurzolo, C., Le Bivic, A., and Rodriguez-Boulan, E. (1994). Cell surface biotinylation techniques. In: Cell Biology: A Laboratory Handbook. San Diego, CA: Academic Press, Inc., 185–192.